# Critical Invalidation of Temperature Dependence of Nanofluid Thermal Conductivity Enhancement

**Kisoo Han**
Mechanical Engineering Department,
Kyung Hee University,
Yongin 449-701, South Korea

**Wook-Hyun Lee**
Korea Institute of Energy Research,
Daejon 305-343, South Korea

**Clement Kleinstreuer**
Mechanical and Aerospace
Engineering Department,
North Carolina State University,
Raleigh, NC 27695-7910

**Junemo Koo**[1]
Mechanical Engineering Department,
Kyung Hee University,
Yongin 449-701, South Korea
e-mail: jmkoo@khu.ac.kr

*Of interest is the accurate measurement of the enhanced thermal conductivity of certain nanofluids free from the impact of natural convection. Owing to its simplicity, wide range of applicability and short response time, the transient hot-wire method (THWM) is frequently used to measure the thermal conductivity of fluids. In order to gain a sufficiently high accuracy, special care should be taken to assure that each measurement is not affected by initial heat supply delay, natural convection, and signal noise. In this study, it was found that there is a temperature limit when using THWM due to the incipience of natural convection. The results imply that the temperature-dependence of the thermal conductivity enhancement observed by other researchers might be misleading when ignoring the impact of natural convection; hence, it could not be used as supporting evidence of the effectiveness of micromixing due to Brownian motion. Thus, it is recommended that researchers report how they keep the impact of the natural convection negligible and check the integrity of their measurements in the future researches.* [DOI: 10.1115/1.4023544]

*Keywords: transient hot-wire method, thermal conductivity, nanofluids, natural convection*

## 1 Introduction

Ever since the report of the *abnormal* thermal conductivity enhancement of nanofluids by Choi and Eastman [1], many researchers have tried to explain the mechanisms leading to extraordinarily high thermal conductivity. Keblinski et al. [2] and Kleinstreuer and Feng [3], among others, discussed several possible explanations such as the effects of enhanced micromixing due to Brownian motion, nanoparticle clustering, layering of fluid molecules on the surface of nanoparticles, and the ballistic transport of phonons in particles. Accordingly, several theories with an emphasis on different thermal nanofluid mechanisms have appeared to predict enhanced conductivity measurements. For example, Koo and Kleinstreuer [4] focused on the impact of nanoparticle Brownian motion with two empirical functions to accommodate temperature and particle interaction effects. Prasher et al. [5] elucidated the impact of the particle clustering and percolation. Kleinstreuer and Li [6] discussed the correlations employed by Jang and Choi [7]. Patel et al. [8] proposed a simple polynomial to match some $k_{\text{nanofluid}}$ measurements. Kleinstreuer and Feng [9] derived a predictive $k_{\text{nanofluid}}$ model without resorting to empirical constants and experimental correlations. The predictive models were developed using the experimentally measured nanofluid thermal conductivity data provided by many research groups.

There are many ways to measure the thermal conductivity of fluids, such as the cylindrical cell method, temperature oscillation method, steady-state parallel-plate method, $3\omega$ method, thermal constants analyzer method, thermal comparator method, and transient hot-wire method. Paul et al. [10] reported that the THWM had been mostly used by nanofluid researchers because of its simplicity and short response time; thereby avoiding the impact of natural convection.

However, there have been large deviations between the effective thermal conductivity measurements of nanofluids, which may originate from differences in the way of data-processing as well as the setup of the test section. Among them, the removal of the natural convection effect was not considered seriously before, but it became one of the key issues among researchers recently. Recalling the fact that the source of the natural convection is the existence of the gravitational acceleration together with the density difference in the momentum equations, the complete elimination might be possible by conducting the measurements in micro- or no-gravity, which would be presently cost-prohibitive. Therefore the management of the natural convection effect on the measurement is inevitable. Recently, Assael et al. [11] reviewed the historical evolution of the transient hot-wire technique, where the importance of the natural convection effect removal was stressed by numerous contributors. Gross et al. [12] measured the thermal conductivities of various refrigerants and they reported the deviations in the positive range due to the natural convection at high temperature. As it was reported by Hong et al. [13], the later part of the temperature history is apt to be affected by natural convection, which leads to the overestimation of the thermal conductivity. They identified the onset of the natural convection comparing the estimated thermal conductivities by varying the start time of the temperature history. By delaying the start time of the temperature history used for thermal conductivity measurements, the estimated thermal conductivity will increase more if the end time lies beyond the time of the onset of natural convection. The point where the lines of the thermal conductivity estimation of different start times meet is called as the crossover point beyond which the impact of natural convection on the measured thermal conductivity cannot be neglected. They suggested that the temperature data range should be selected with caution so that the impact of natural convection remains negligible. Vadasz et al. [14] scrutinized the possible explanations for observed thermal conductivity

[1]Corresponding author.

Contributed by the Heat Transfer Division of ASME for publication in the Journal of Heat Transfer. Manuscript received August 15, 2012; final manuscript received January 18, 2013; published online April 11, 2013. Assoc. Editor: Oronzio Manca.

  

**Table 1 Temperature dependence of the thermal conductivity increase observed by other researchers**

| Authors (method) | Particle materials | Size (nm) | Base fluids | $\phi_{max}$ (vol. %) | $T$ (K) | $k$-$T$ relation |
|---|---|---|---|---|---|---|
| Jang and Choi [23] | $Al_2O_3$ | 38.4 | Water | 1.0 | 300–325 | Increase |
| | CuO | 6 | Water | 1.0 | 300–325 | Increase |
| Das et al. [24] | $Al_2O_3$ | 38.4 | Water | 1.0 | 293–323 | Increase |
| | $Al_2O_3$ | 38.4 | Water | 4.0 | 293–323 | Increase |
| | CuO | 10 | Water | 1.0 | 298–328 | Increase |
| Prasher [25] | $Al_2O_3$ | 12 | Water | 4.0 | 293–323 | Increase |
| Chon and Kihm [26] | $Al_2O_3$ | 11 | Water | 3.0 | 293–333 | Increase |
| | $Al_2O_3$ | 47 | Water | 3.0 | 293–333 | Increase |
| | $Al_2O_3$ | 150 | Water | 3.0 | 293–333 | Increase |
| Murshed et al. [27] | $Al_2O_3$ | 80 | EG | 1.0 | 293–333 | Increase |
| Mintsa et al. [28] (KD2) | $Al_2O_3$ | 36, 47 | Water | 18 | 293–323 | Increase |
| | CuO | 29 | Water | 14 | 293–313 | Increase |
| Duangthongsuk and Wongwises [29] (THWM) | $TiO_2$ | 21 | Water | 2.0 | 288–308 | Increase |
| Vajjha and Das [30] (THWM) | $Al_2O_3$ | 53 | EG–Water mixture | 10 | 298–363 | Increase |
| | CuO | 29 | EG–Water mixture | 6 | 298–363 | Increase |
| | ZnO | 29, 77 | EG–Water mixture | 7 | 298–363 | Increase |
| Teng et al. [31] (KD2) | $Al_2O_3$ | 20, 50, 100 | Water | 0.5 | 283–323 | Increase |
| Turgut et al. [32] ($3\omega$) | $TiO_2$ | 21 | Water | 3 | 286–328 | Independent |
| Shima et al. [33] (KD2 Pro) | $Fe_3O_4$ | 8 | Kerosene, hexadecane, water | 9.5 | 298–323 | Independent |
| Lee et al. [34] (THWM, lambda) | ZnO | 70 | EG | 5.5 | 293–363 | Mostly decrease |

enhancements, and they pointed out the importance of properly selecting the "valid range of data reduction" to mitigate the impact of natural convection.

Natural convection is an important issue not only for the thermal conductivity measurements but also for the heat transfer enhancement. Concerning nanofluids used for cooling, there are contradictory theories about the influence of natural convection. Putra et al. [15], Li and Peterson [16], Ni et al. [17] and Donzelli et al. [18] experimentally investigated the natural convection of water-based $Al_2O_3$ and CuO nanofluids and observed the deterioration in heat transfer. Corcione [19], Hwang et al., [20] and Kim et al. [21] performed a theoretical study and concluded that the nanofluids are more stable than pure liquids due to the increased viscosity. In contrast, Tzou [22] investigated analytically the thermal instabilities of nanofluids and reported the decrease of critical Rayleigh number and hence the heat transfer enhancement. Hong et al. [13] observed the earlier incipience of natural convection for nanofluids when compared to pure fluids when measuring thermal conductivities. The thermal conductivities of base fluids such as water and ethylene glycol (EG) increase with temperature. Hence, the change of the nondimensional thermal conductivity enhancement ($k_{nanofluid}(T)/k_{basefluid}(T)$) with temperature has been investigated by many researchers. Table 1 lists the temperature-dependence of nanofluid thermal conductivity enhancement observed by researchers. Most research groups in the table [23–31] found an increase of thermal conductivity enhancement with temperature for nanofluids. They mostly tried to explain this resorting to the impact of Brownian motion which is believed to be more effective with temperature increase. Some researchers reported that the thermal conductivity enhancement remained constant, i.e., independent of temperature [32,33] or even decreased with temperature [34].

As shown above, it has been reported that there were deviations between the effective thermal conductivity measurements from different research groups. Although Hong et al. [13] and Vadasz et al. [14] have pointed out that the selection of temperature history range could affect the estimation of the nanofluid thermal conductivity; they did not test that directly. In this study, the thermal conductivities of water and EG as well as nanofluids were measured using THWM, excluding the impact of natural convection for the temperature range 293–338 K. The results were compared with the cases of improper selections of temperature history. It was found that the temperature dependence of the nanofluid thermal conductivity enhancement could be a mistake due to improper selections of temperature data range affected by natural convection. Furthermore, it was found that there existed the temperature limits in THWM application due to the onset of the natural convection.

## 2 Theory

**2.1 Principles of Transient Hot-Wire Method.** To measure the thermal conductivity of fluids using THWM, electric power is introduced to the hot-wire where it is converted to heat which increases the hot-wire temperature, but is also partly dissipated into the surrounding fluid via heat conduction. The amount of heat and the thermal conductivity of the surrounding fluid determine the temperature changes in the wire. For fluids of high thermal conductivities, the heat dissipates well and hence results only in a small hot-wire temperature rise. In contrast, higher hot-wire temperatures can be expected when the surrounding fluid's thermal conductivity is small. The thermal conductivity of the fluid is measured under the assumption that heat transfer occurs only in the conduction mode. The relation between the hot-wire temperature history and the thermal conductivity of the fluid is given by Carslaw and Jaeger [35] as

$$k_f = \frac{\dot{Q}}{4\pi L_w} \cdot \frac{d \ln t}{dT_w} \tag{1}$$

Figure 1 shows an example of temperature data taken with the THWM apparatus. The open circle symbols represent the temperature data at the corresponding time shown. The series of wire temperature data taken in time is known as the "temperature history." The thermal conductivity is evaluated using Eq. (1) where the gradient term is the reciprocal of the slope in the time range between the "start time" and "end time" applying the least square method. Because the wire temperature cannot be directly measured, the change in the wire's electric resistance is measured and then the temperature is estimated using the following equation:

$$R_w = R_0(1 + \alpha T_w) \tag{2}$$

Measuring the change in wire resistance $R_w$ with time and converting it to the wire temperature using Eq. (2), the thermal conductivity of the fluid can be estimated with Eq. (1).

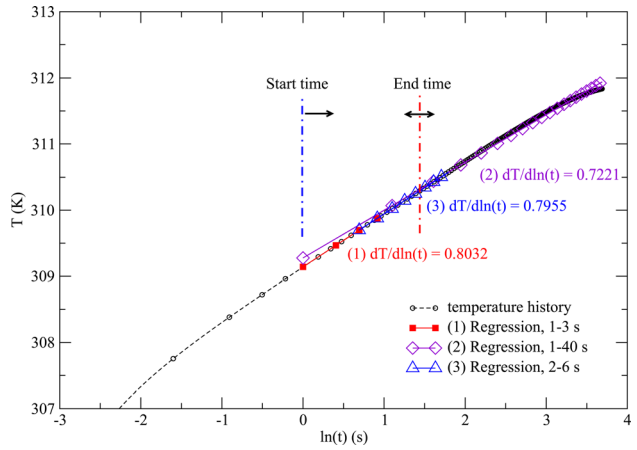


**Fig. 1 Definitions of temperature history, start- and end-time in the data**

**2.2 Natural Convection in Test Section.** As the hot-wire temperature increases due to the Joule heating effect, the temperature difference between the hot-wire surface and the bulk fluid increases. The temperature difference generates a buoyancy force due to the density difference between the fluid on the hot-wire surface and the bulk fluid, which is balanced by the viscous force in the early stage. As the temperature difference increases past a critical value with the elapse of heating time, the buoyance force exceeds the viscous force and natural convection starts to occur in the test cell. As in addition to heat conduction also natural convection comes into play in the course of thermal conductivity measurements using THWM, the hot-wire generating heat will be removed to the surrounding fluid more rapidly. The increased heat transfer rate will result in a smaller hot-wire temperature rise over time, which will lead to an increase in the gradient term in Eq. (1), resulting in an overestimation of the thermal conductivity. Therefore, it is necessary to restrict the end time of the temperature history used for data processing to the point where measurements are not affected by natural convection. In order to determine the unaffected region, thermal conductivities are measured by varying the start- and end-times. The slopes in Fig. 1 decrease when taking the temperature history data at a later part which is affected by natural convection. As the start time delays, the impact of natural convection on the thermal conductivity becomes stronger and the slope becomes smaller for a fixed end time. To identify the point where the natural convection effect comes into play, the following procedure has been used. First, thermal conductivities are obtained for different end-times, keeping the start-time fixed. Then, the thermal conductivities are estimated for varying start-times. With larger start-times the slope of the increasing thermal conductivity increases as well, generating "cross-over points" beyond which the effect of natural convection cannot be ignored. Thus, any temperature data beyond the crossover points should be effectively eliminated (see Ref. [13]).

The effect of thermal property variation of working fluids by adding nanoparticles on the natural convection was investigated applying the conventional natural heat transfer theory. The thermal properties of EG-based 1.0% ZnO nanofluids were measured to be about 4% higher for the density, 30% lower for the thermal expansion coefficient, 0.7% higher for the viscosity, 5% higher for the thermal conductivity than those of pure EG. Although the heat capacity has not been directly measured, it can be assumed that its volume-fraction weighted average is higher by 0.4%. Estimating the changes in Rayleigh number as given in Eq. (3), it is lower by 67% when compared to pure EG, indicating the deterioration of natural convection referring to the conventional theory (see Ref. [13]).

$$\mathrm{Ra} = g\Delta T\left(\frac{\beta}{\mu}\frac{\rho^2 c_\mathrm{p}}{k}\right) \tag{3}$$

In this study, the incipience time of natural convection was directly identified without the necessity of material property models and Rayleigh number relation. Thus, unlike other theoretical and numerical researches, the observations in this study are free from the errors in the property prediction models and the limits of conventional natural convection theory.

## 3 Experimental Setup

**3.1 Apparatus Setup.** Figure 2 shows the schematics of the transient hot-wire apparatus. A dc power supplier (array, model 3654A, Korea) imposed 4 V across the Wheatstone bridge. The switching of the power supply was controlled by a relay circuit to avoid any delay effect. The initial resistances of the resistors and the hot wires were measured by a low resistance meter (GoodWill, model GOM-801 G), which had a maximum reading error of 0.2%. The test section of 141 mm length and 12 mm radius was fabricated with acrylic pipe, and the top and bottom sides were covered by the lids made of polyvinyl acetal. The hot-wire was made of 50 $\mu$m diameter platinum coated by a 25 $\mu$m electrically insulating Teflon layer. A thinner wire with anodic coating layer could be used to reduce the impacts of both the initial delay and the insulation layer; however, the thicker wire was used due to the ease of handling. The time variations of the voltage drop across the whole Wheatstone bridge and the voltage difference between the midpoints of the Wheatstone bridge circuit were stored in the computer using a data acquisition system (National Instrument, model USB-6210). A special grade *k*-type thermocouple from Omega Engineering, Inc., which has the accuracy of 0.4% or 1.1 K whichever is greater (0.75% or 2.2 K whichever is greater for standard grade) with the measuring range of 73–1253 K was installed near the outer wall to monitor the bulk fluid temperature near the test section wall as shown in Fig. 2. It was necessary to check if the bulk fluid temperature would reach the set surrounding temperature in the constant temperature chamber, where the test section was located to perform the thermal conductivity measurements.

Roder et al. [36] reported that the incipience of natural convection occurs at the critical Rayleigh number ($\mathrm{Ra}_{\mathrm{crit}} = g\beta\Delta T(r_w - r_0)^3/\alpha\nu$). Assuming the constant values of the critical Rayleigh number and material properties, the onset of natural convection could vary depending on the applied power to the hot-wire. The temperature difference $\Delta T$ is smaller for smaller power input, which will delay the onset of natural convection. In contrast, the measurement will suffer more from the signal noise in that case. In this study, the proper level of the input power was determined to be 4 V from the experimental test, where shows the effect of the applied voltage on the noise level and measurement accuracy are as shown in Table 2.

**3.2 Material Preparation.** Water-based Ag and EG-based ZnO nanofluids were prepared by the one-step method in the Korean Institute of Energy Research (KIER). They were redispersed by applying ultrasonication for 3 h using a bar-type sonicator. Figure 3 shows the scanning electron microscope (SEM) images of Ag and ZnO nanoparticles prepared by evaporating the base fluid. Since the suspended particle volume fraction could vary in time, the particle volume fractions were estimated by measuring the specific gravity of the nanofluids, using an electronic hydrometer (GP-300S, Matsuhaku, Japan). Then, the volume fractions were obtained by the following equation:

$$\phi = \frac{\rho_\mathrm{n} - \rho_\mathrm{f}}{\rho_\mathrm{p} - \rho_\mathrm{f}} \tag{4}$$

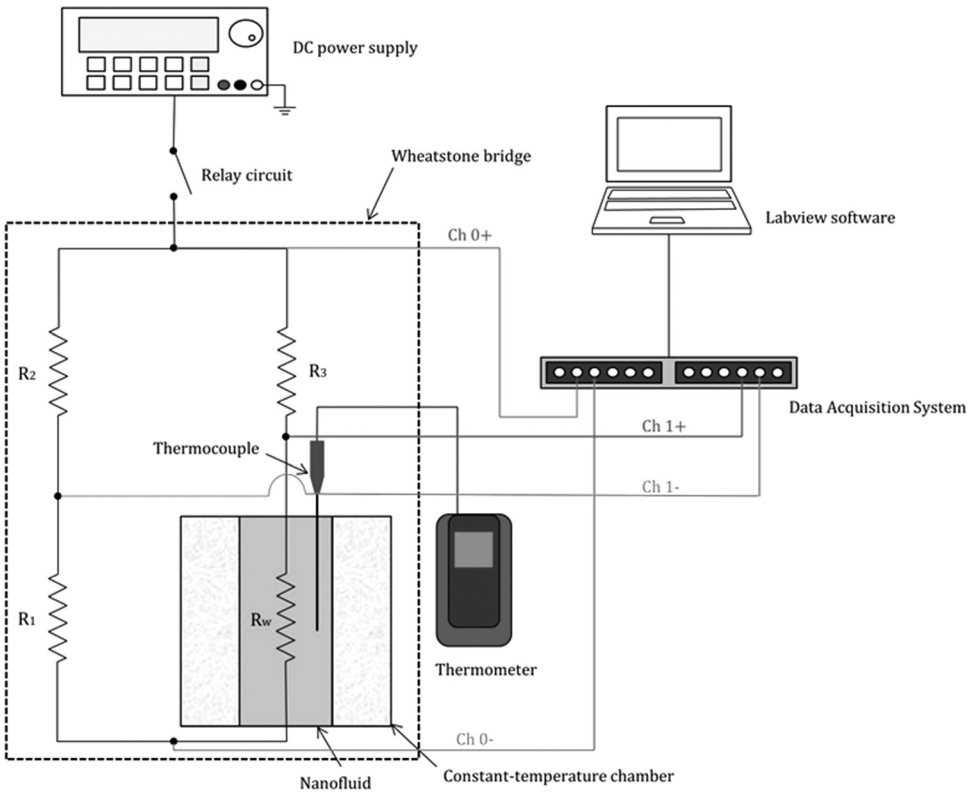


**Fig. 2 Schematics of the apparatus for data collection using the transient hot-wire method**

**Table 2 The effects of applied voltage on the thermal conductivity measurement errors and noise levels**

| Fluid | Voltage (V) | Thermal conductivity (W/mK) | Thermal conductivity error (%) | Noise, min.–max. (mV) | Noise error (%) |
|---|---|---|---|---|---|
| Water | 2 | 0.5913 | −3.42 | 0.823 | 0.041 |
| | 3 | 0.6056 | −1.06 | 0.822 | 0.027 |
| | 4 | 0.5973 | −2.45 | 0.988 | 0.024 |
| | 5 | 0.6103 | −0.32 | 0.822 | 0.016 |
| | 6 | 0.6051 | −1.17 | 1.645 | 0.033 |
| EG | 2 | 0.2601 | −3.34 | 1.115 | 0.043 |
| | 3 | 0.2613 | −3.83 | 1.116 | 0.033 |
| | 4 | 0.2558 | −1.60 | 1.114 | 0.023 |
| | 5 | 0.2613 | −3.71 | 1.116 | 0.029 |
| | 6 | 0.2567 | −2.02 | 1.645 | 0.027 |

With the particle and liquid densities known, that of each nanofluid could be estimated from the specific gravity measured by the hydrometer.

The solubility of air in a base fluid decreases with temperature, so that bubbles form on the wire surface and walls when the experiments are performed in the order of increasing temperature. The bubbles act as thermal resistances and hamper the exact measurement of the thermal conductivity. Hence, the degasification of base fluids and nanofluids is very important. There are many ways to perform the degassing including pressure reduction, heating, freeze-pump-thawing and sonication. The pressure reduction uses the virtue of Henry's law which states that the amount of the dissolved gas in equilibrium is in proportional to the partial pressure of the gas, and the heating takes advantage of the solubility decrease with the increase of liquid temperature. The outgassing process was done by simply raising fluid temperature to 338 K which is the highest possible temperature of the temperature control chamber in the lab could manage, and lower down to the highest temperature to measure the thermal conductivities and performed the measurements in the descending temperature manner. Traditionally, outgassing is performed by boiling the liquid. For nanofluids, the boiling process usually ends up with undesirable particle aggregation. When bubbles were noticed on the wire surface without the degasification in the pure fluids, the measurements resulted in lower thermal conductivity than those of base fluids. With the degasification process, the bubbles were not observed even after a long storage time in the test cell, and the thermal conductivity measurements of pure fluids repeatedly and precisely matched the literature values. The nanofluids experienced an additional degasification process due to the 3 h sonication process in the preparation stage, where the temperature rose quite high and the bubbles would be detached and removed during the process due to the pressure wave.

**3.3 Data Processing.** The temperature data were obtained for the time range of 0–20 s, while the data in the range of 0–1 s were truncated to eliminate the finite wire heat capacity effect. The data affected by natural convection were removed using the method outlined in Sec. 2.2 (see also Ref. [13]). The thermal

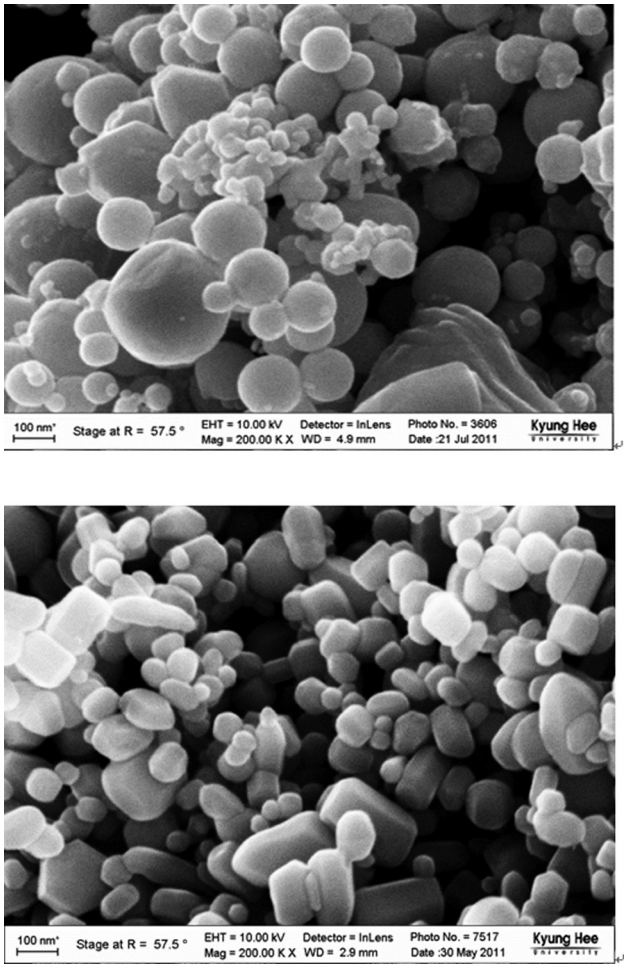


**Fig. 3 SEM images of nanoparticles used in the nanofluids**

conductivity of a fluid was statistically estimated out of 13 temperature data sets per measurement. The measurements of the effective thermal conductivities of nanofluids were compared with those of the base fluids and the conventional thermal conductivity models.

## 4 Results and Discussion

**4.1 Uncertainty Analysis of the Measurements.** The confidence interval on the mean of a random sample could be obtained using the following equation:

$$\bar{X} = \mu + T_{\alpha/2,n-1}\frac{S_x}{\sqrt{n}} \tag{5}$$

where $\alpha$ is the significance level of the test. The total uncertainty is composed of the bias and precision errors, where the bias error is defined as the difference between the mean and the sampled mean, and precision error as the half interval in which 95% of sampled data fall in.

The uncertainty analysis results are shown in Table 3. The maximum uncertainty was found to be about 2%. The uncertainty level was slightly greater for the case of water, and it tended to increase with fluid temperature. It was evident that water at high temperature is impacted more by natural convection due to its low viscosity and high volume expansion coefficient. The measured thermal conductivities were compared with the reference values by using the hypothesis test to check the statistical difference. The measurements were found to be statistically not different from the reference values.

**4.2 Upper Temperature Limits for Thermal Conductivity Measurements.** Figures 4(*a*)–4(*d*) depict the crossover points and measuring points after data processing. The hot-wire temperature changes with time due to the Joule heating effect. As was pointed out by Hong et al. [13], the estimated thermal conductivity values oscillate near the start-time where the data range selected is short and the estimation is sensitive to the local noise. The oscillation originates from the signal noise, which vanishes or averages out with the extension of the end time. Then, the estimated thermal conductivity values reach a local minimum, where the end time for the measurements is assigned. Thermal conductivity estimations at later starting times are higher due to the stronger effect of natural convection, making the crossover point. The crossover points of (a) pure water and (b) water-based Ag nanofluids were observed at 313 K to be 3.92 and 2.72 s, respectively. Those of (c) pure EG and (d) EG-based ZnO nanofluids at 303 K were measured to be 8.75 and 5.77 s, respectively. The measurement times were for test: (a) 1.7–3.2 s, (b) 1.5–2.8 s, (c) 1.7–5.8 s, and (d) 1.5–4.8 s. Although the onset times for nanofluids were expected to be delayed, considering the increase of viscosities and the decrease of thermal expansion coefficients, those of nanofluids were observed to occur earlier than those of pure fluids. This is contrary to the conventional theory. The phenomenon might be interpreted as evidence of a new transport mechanism by nanoparticles in liquids. According to Tzou [22], the heat transfer improves with inclusion of nanoparticles enhancing the fluid mixing. The exact mechanism is not clear yet, whether it is due to Brownian motion, thermophoresis or osmophoresis.

Figure 5 shows the intervals between the temperature-measuring points and crossover points, which represent the margins of measurements, i.e., the intervals between the blue square and the red circle symbols in Fig. 4. The measuring points were determined considering two conditions. There should be enough duration past the start-time for the signal noise to average out, and the estimation should generate a local minimum (or a plateau) before the crossover point. If natural convection affects the measurements from the very early stage of the measurements, the measuring point cannot be placed, which implies measurement failure. Hence, that margin is a very important factor to set the high temperature limit of the THWM apparatus. The margin of measurement for water decreased from 2.58 s at 293 K to 0.29 s at 338 K, while it reduced from 2.46 s to 0.13 s under the same conditions for water-based Ag nanofluids.

**Table 3 Uncertainty analysis of the measurements**

| | Temperature (K) | | | | | | | | | | | |
|---|---|---|---|---|---|---|---|---|---|---|---|---|
| | Water | | | | | | Ethylene glycol | | | | | |
| | 293 | 303 | 313 | 323 | 333 | 338 | 293 | 303 | 313 | 323 | 333 | 338 |
| Bias error (%) | 0.96 | 0.30 | 0.57 | 0.24 | 0.34 | 0.40 | 0.65 | 0.96 | 0.69 | 0.18 | 0.44 | 0.08 |
| Precision error (%) | 0.71 | 1.40 | 0.90 | 1.92 | 1.78 | 1.84 | 0.21 | 0.42 | 0.38 | 0.39 | 1.59 | 1.11 |
| Total uncertainty (%) | 1.67 | 1.70 | 1.47 | 2.16 | 2.11 | 2.23 | 0.86 | 1.38 | 1.06 | 0.57 | 2.03 | 1.19 |

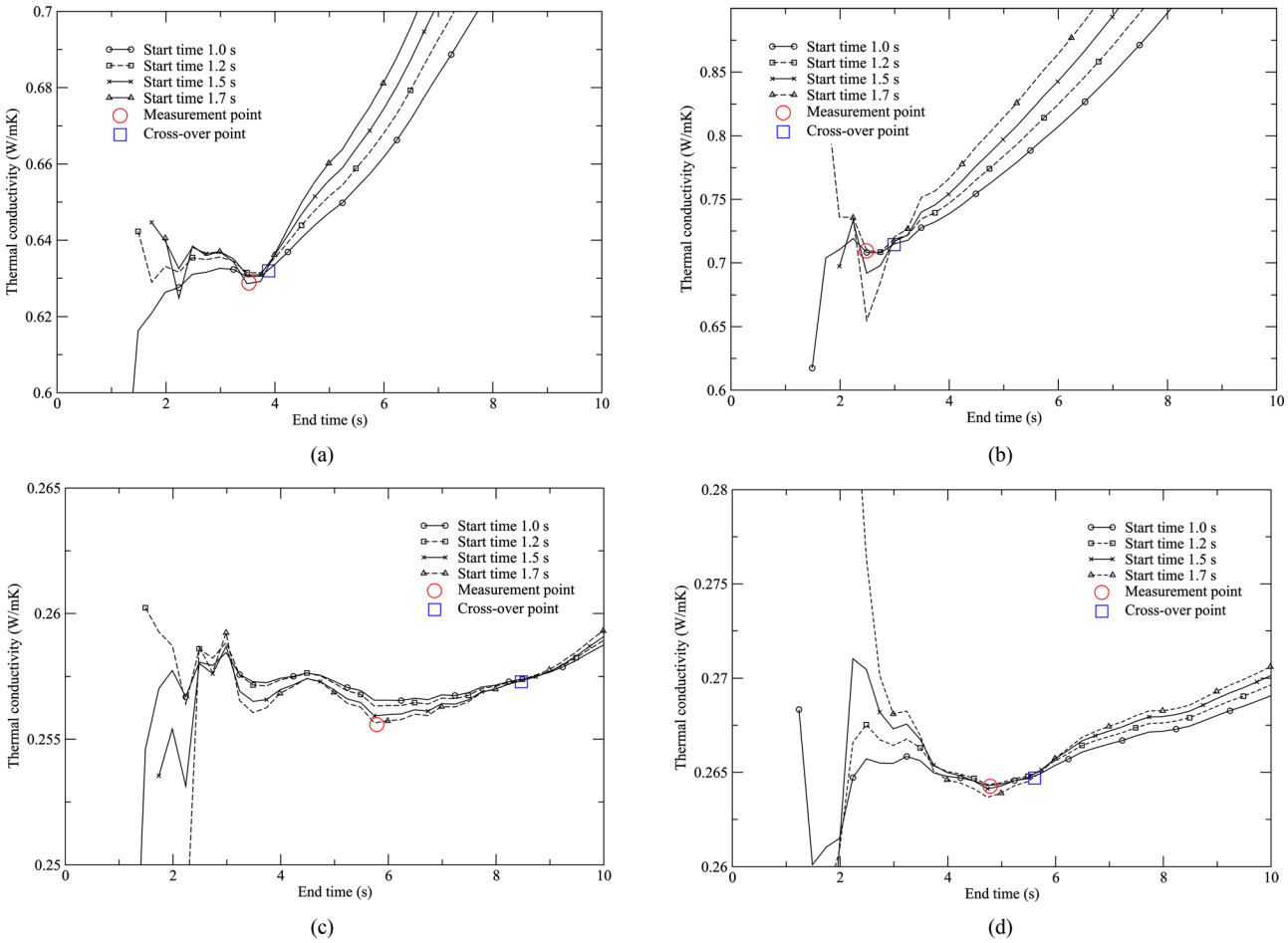


**Fig. 4 Effects of temperature data-range selections on thermal conductivity determination for: (*a*) water; (*b*) water-based Ag nanofluid at 313 K; (*c*) EG; and (*d*) EG-based ZnO nanofluid at 303 K**

As the temperature increases, the measuring point approaches the crossover point. In the case of water and water-based Ag nanofluids the two points practically coincided at 338 K, indicating the upper temperature limit of thermal conductivity measurement for these fluids. For EG and EG-based ZnO nanofluids at 338 K there were larger margins, i.e., 0.71 s and 0.44 s, respectively. Therefore, the upper temperature limit of thermal conductivity measurements for water and water-based Ag nanofluids was found to be 338 K, whereas the limits for EG and EG-based ZnO nanofluids were a little higher. The actual temperature limits for EG and EG-based nanofluids could not be exactly determined because the maximum temperature limit of the temperature control chamber used was 338 K.

**4.3 Temperature-Dependence of Nanofluids Thermal Conductivity Enhancement.** Figure 6 shows the thermal conductivity measurements of nanofluids ($k_{nanofluid}$) as well as pure

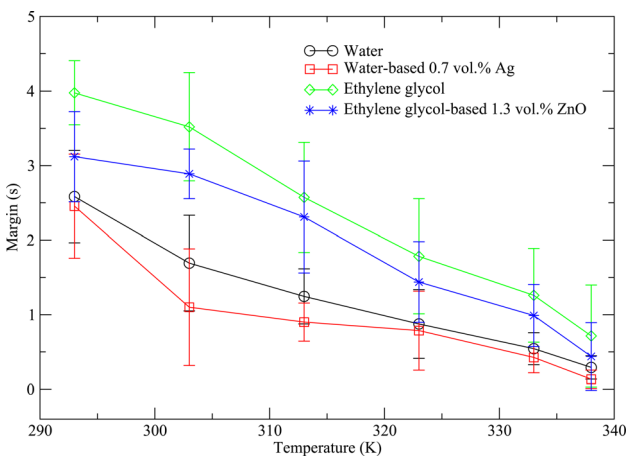


**Fig. 5 Comparison of measurement margins for different fluids**

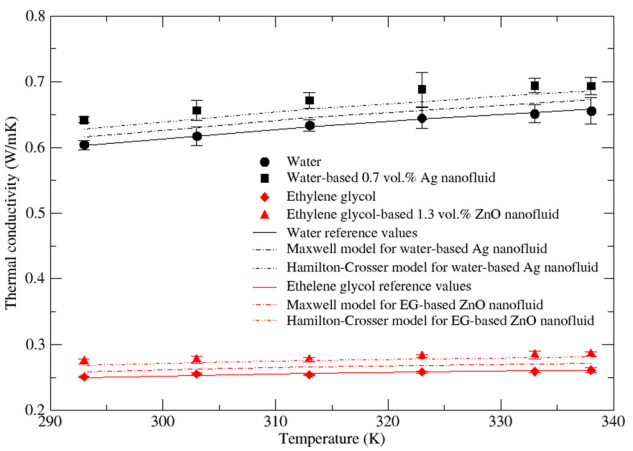


**Fig. 6 Comparison of thermal conductivity measurements between pure base fluids and nanofluids versus the predictions by Maxwell's model**

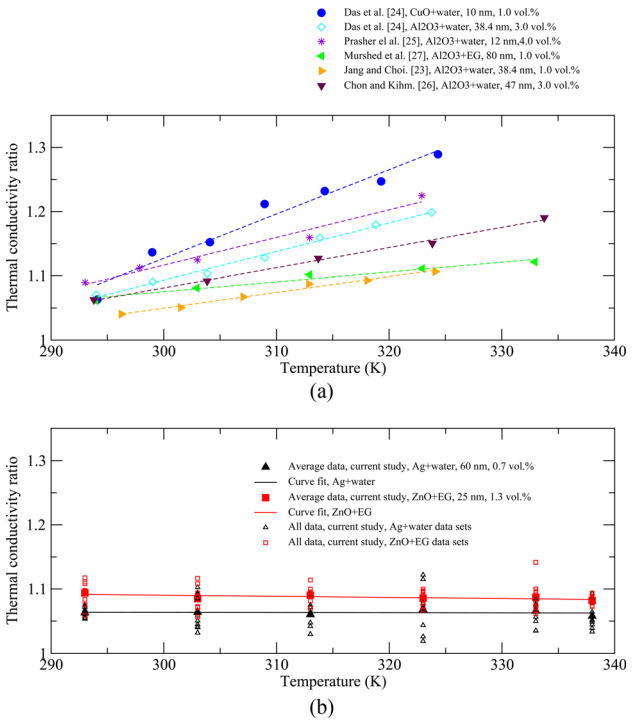


**Fig. 7 Comparison between research groups concerning the temperature dependence of effective thermal conductivity enhancement of nanofluids: (*a*) other groups; and (*b*) current study**

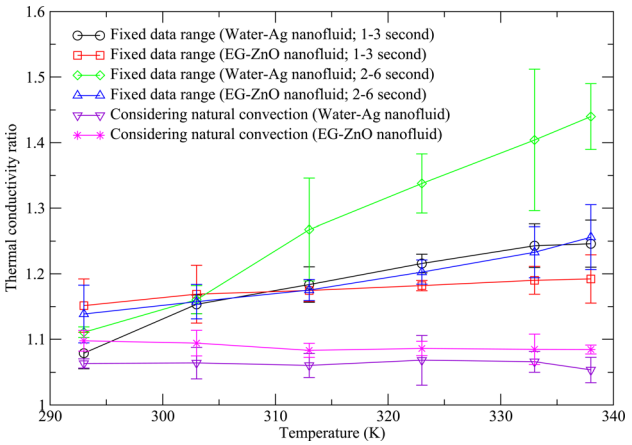


**Fig. 8 Effect of temperature data-range selection on the estimation of the nanofluid effective thermal conductivity**

fluids ($k_{\text{basefluid}}$) together with the thermal conductivity predictions of nanofluids using the Maxwell and Hamilton & Crosser models. As mentioned, the measurements of the pure fluids, i.e., water and EG, were statistically validated using the hypothesis test, i.e., they were not different from the reference values. The thermal conductivities of both pure fluids and nanofluids were observed to increase with temperature and for the nanofluids being above the predictions of the Maxwell and Hamilton and Crosser models.

The laboratory data sets were statistically investigated to check whether there was a temperature dependence of the thermal conductivity enhancement of nanofluids over predictions by conventional theory. The measured thermal conductivity ratios and published data sets are shown in Figs. 7(*a*) and 7(*b*). It has been reported that, indeed, the $k_{\text{nanofluid}}/k_{\text{basefluid}}$ ratio increases with temperature, where some researchers obtained temperature data during a fixed time range [37–39], e.g., 1–3 s, while others did not provide any details concerning the selected temperature and time ranges. When employing a fixed time range, the thermal conductivity measurements are prone to be affected by natural convection; because, the onset of natural convection occurs earlier with increasing fluid temperature, resulting in an overestimation of the thermal conductivity. Figure 7(*a*) represents the reported measurements from other researchers showing the increase of thermal conductivity enhancement with temperature. In this study, the thermal conductivity enhancement of nanofluids was found to be independent of fluid temperature after effectively removing the impact of natural convection by using the technique outlined in Sec. 2.2 as shown in Fig. 7(*b*). Figure 8 shows the effects of data-range selection on thermal conductivity determination. The thermal conductivities were measured both by the newly developed method to avoid the impact of natural convection as well as the technique using the temperature data in fixed time ranges. The thermal conductivity enhancement of nanofluids was found to increase with temperature when using temperature data in fixed time ranges. The increase with temperature was found to be stronger for the cases using temperature data in the later time range, i.e., 2–6 s in Fig. 8. This could be explained from the fact that the incipience of natural convection occurs earlier with temperature due to the decrease in fluid viscosity and increase in thermal expansion coefficient. The changes in viscosity and thermal expansion coefficient with temperature were greater for water than for EG; thus, water-based nanofluids were prone to be affected by natural convection (see Fig. 4). The thermal conductivities of water-based nanofluids were always greater when using the temperature data in the time range of 2–6 s, and they were still greater than the cases of measuring the thermal conductivities considering the removal of the natural convection effect. In cases of EG-based nanofluids, the incipience of natural convection appeared at a later time than for the cases of water-based nanofluids. In fact, for thermal conductivities measured between 293 and 313 K there was statistically no difference between the two different selections of temperature data ranges. After that the thermal conductivity measurements of the cases using temperature data in 2–6 s were slightly greater than the cases using the data in 1–3 s interval. The thermal conductivity enhancement measurements using a fixed time range were much greater than when removing the natural convection effect.

In contrast to observations by other researchers (see Table 1), the present thermal conductivity values were found to be independent of fluid temperature, as based on statistical analysis (see Ref. [40]). The temperature independence of the measurements was tested by F-test for the regression expressions of the $k_{\text{nanofluid}}/k_{\text{basefluid}}$ ratio data. The regression expressions for water-based 0.7 vol. % Ag nanofluid and EG-based 1.3 vol. % ZnO nanofluid were obtained as

$$\frac{k_{\text{water-based Ag nanofluid}}}{k_{\text{basefluid}}} = -3.619 \times 10^{-5} T + 1.074 \qquad (6)$$

and

$$\frac{k_{\text{EG-based ZnO nanofluid}}}{k_{\text{basefluid}}} = -1.866 \times 10^{-4} T + 1.147 \qquad (7)$$

The results of the t-test for the null hypothesis, i.e., "the model is not significant," are summarized in Table 4. In this table, total sum of squares (SST), sum of squared errors (SSE), and residual

**Table 4 The results of F-test to check statistically the temperature dependence of the thermal conductivity increase with temperature with the confidence level of 95%**

| Nanofluids | SST | SSE | SSR | Reject | *F*-value | Results |
|---|---|---|---|---|---|---|
| Water/Ag | 0.025 | 0.025 | $1.68 \times 10^{-5}$ | 4.03 | 0.033 | Not significant |
| EG/ZnO | 0.014 | 0.014 | $5.05 \times 10^{-4}$ | 3.84 | 2.099 | Not significant |

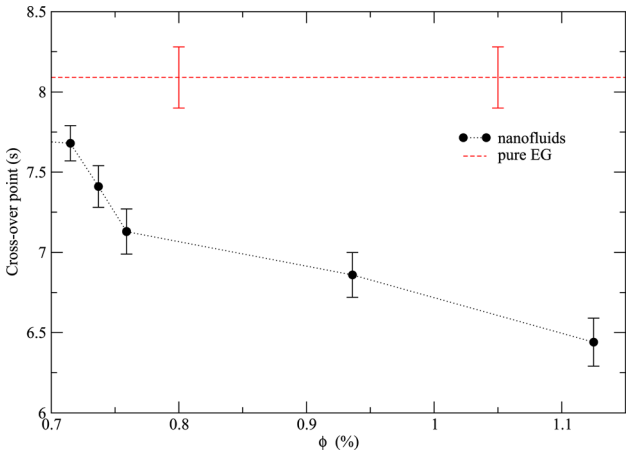


**Fig. 9 Effect of particle volume fraction on the incipience of natural convection for EG-based ZnO nanofluids**

sum of squares (SSR) represent the total, error and regression sums of squares, and the test compares the ratio between SSR and SSE. If the ratio, F-value in Table 4, is greater than a certain value under a given significance level, the values in the "Reject" column in Table 4, the null hypothesis is rejected, otherwise it cannot be rejected, meaning no difference. Comparing the SSR and SSE, the variation due to temperature change was found to be negligible comparing with other uncertainties in measurements. One possible reason is that the observations by others may have been affected by an earlier inception of natural convection with rising temperature.

Figure 9 shows the effect of the particle volume fraction on the incipience of natural convection for EG-based ZnO nanofluids. The crossover point advanced with the addition of ZnO nanoparticles. The crossover point for pure EG was at about 8.1 s; it occurred earlier at about 6.5 s with ZnO volume fraction about 1.1%. This clearly shows that the addition of particles for the tested range advances the onset of natural convection.

The effective thermal conductivity measurements against the volume fraction are given in Fig. 10. The measured data are shown as circles with error bars indicating the standard deviations of the measurements. The lines represent the conventional estimations of the thermal conductivity using the Maxwell relation with the size-dependent particle conductivities given in Morkoç and Özgür [41]. Clearly, thermal conductivity enhancement was still above the estimations when using the Maxwell relation, and it increased with particle volume fraction. The thermal conductivity enhancement is a concave function, decreasing the enhancement rate with particle concentration.

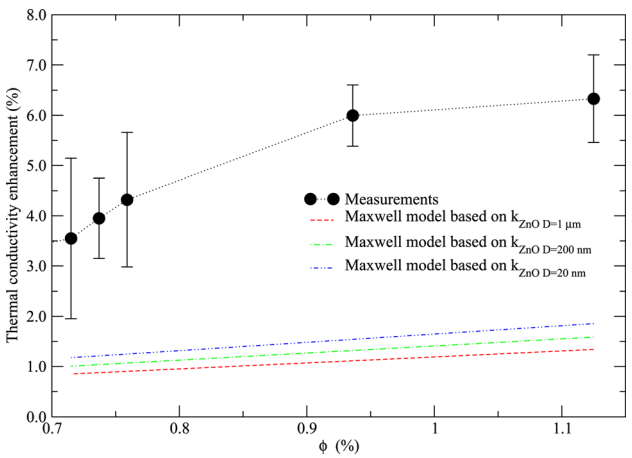


**Fig. 10 Thermal conductivity enhancement with the variation of the ZnO particle volume fraction in EG-based nanofluids**

## 5 Conclusions

Using the transient hot-wire method, the upper temperature limit to accurately measure the thermal conductivities of liquids and nanofluids was identified by comparing the natural convection onset point and actual temperature-measuring point. The thermal conductivities of the pure fluids (i.e., water and EG) as well as the nanofluids (i.e., water-Ag and EG-ZnO) were measured and compared. The following conclusions can be drawn from this study:

(1) As expected, the onsets of natural convection were found to occur earlier with the increase of fluid temperature for both pure fluids and nanofluids.
(2) The high temperature limit of thermal conductivity measurement for the given laboratory set was found to be 338 K for water. Considering the small margin between the measuring point and the crossover point, it is assumed to be a slightly higher for EG.
(3) Onset of natural convection occurred earlier for nanofluids when compared to the corresponding base fluids. This cannot be explained using conventional theory of natural convection, where natural convection weakens with the inclusion of particles due to an increase of viscosity and a decrease in the thermal expansion coefficient.
(4) The thermal conductivity enhancements of the water-based Ag nanofluid with 0.7% volume fraction and the EG-based ZnO nanofluid with 1.3% volume fraction were measured to be 6.3% and 8.2%, respectively.
(5) Both $k_{nanofluid}/k_{basefluid}$ values were found to be statistically independent of temperature. This implies that the increase of the thermal conductivity enhancement with temperature could be a mislead, and it could not be supporting evidence of the Brownian motion effect, although it could still be an important mechanism to explain the thermal conductivity enhancement.
(6) The failure to exclude the impact of natural convection on thermal conductivity measurements was found to be a possible explanation of thermal conductivity enhancement increase with temperature. Thus, it is recommended that the impact of natural convection on thermal conductivity measurements is eliminated.

## Acknowledgment

This work was supported by the National Research Foundation of Korea (NRF) via a grant provided by the Korean Government (MEST) (2010-0024795).

## Nomenclature

EG = ethylene glycol
$g$ = gravitational acceleration (m/s$^2$)
$k$ = thermal conductivity (W/mK)
$L$ = length (m)
$n$ = sample size
$Q$ = amount of heat (J)
$r$ = radius (m)
$R$ = resistance (Ω)
Ra = Rayleigh number
$S$ = standard deviation
SEM = scanning electron microscope
SSE = sum of squared errors
SSR = residual sum of squares
SST = total sum of squares
$t$ = time (s)
$T$ = temperature (K)
THWM = transient hot-wire method
$\bar{X}$ = sampled mean

## Greeks Symbols

$\alpha$ = temperature coefficient of resistivity (0.00362 $K^{-1}$ for platinum wire)
$\alpha$ = significance level of the test
$\beta$ = volume expansion coefficient ($K^{-1}$)
$\Delta$ = difference
$\mu$ = mean
$\nu$ = kinematic viscosity ($m^2/s$)
$\rho$ = density ($kg/m^3$)
$\phi$ = volume fraction

## Subscripts

0 = 0 °C, test cell
f = fluid
n = nanofluid
p = particle
w = wire

## References


[1] Choi, S. U. S., and Eastman, J. A., 1995, "Enhancing Thermal Conductivity of Fluids With Nanoparticles," Developments Applications of Non-Newtonian Flows, D. A. Siginer, and H. P. Wang, eds., FED/MD, ASME, New York, Vol. 231/66, pp. 99–105.
[2] Keblinski, P., Philpot, S. R., Choi, S. U. S., and Eastman, J. A., 2002, "Mechanisms of Heat Flow in Suspensions of Nano-Sized Particles (Nanofluids)," Int. J. Heat Mass Transfer, **45**, pp. 855–863.
[3] Kleinstreuer, C., and Feng, Y., 2011, "Experimental and Theoretical Studies on Nanofluid Thermal Conductivity Enhancement: A Review," Nanoscale Res. Lett., **6**, p. 229.
[4] Koo, J., and Kleinstreuer, C., 2005, "Impact Analysis of Nanoparticle Motion Mechanisms on the Thermal Conductivity of Nanofluids," Int. Commun. Heat Mass Transfer, **32**, pp. 1111–1118.
[5] Prasher, R., Phelan, P. E., and Bhattacharya, P., 2006, "Effect of Aggregation Kinetics on the Thermal Conductivity of Nanoscale Colloidal Solutions," Nano Lett., **6**, pp. 1529–1534.
[6] Kleinstreuer, C., and Li, J., 2008, "Discussion: 'Effects of Various Parameters on Nanofluid Thermal Conductivity' (Jang, S. P., and Choi, S. D. S., 2007, ASME J. Heat Transfer, **129**, pp. 617–623)," ASME J. Heat Trans., **130**(2), p. 025501.
[7] Jang, S. P., and Choi, S. U. S., 2007, "Effects of Various Parameters on Nanofluid Thermal Conductivity," ASME J. Heat Trans., **129**(5), pp. 617–623.
[8] Patel, H. E., Sundararajan, T., and Das, S. K., 2010, "An Experimental Investigation Into the Thermal Conductivity Enhancement in Oxide and Metallic Nanofluids," J. Nanopart. Res., **12**(3), pp. 1015–1031.
[9] Kleinstreuer, C., and Feng, Y., 2012, "Thermal Nanofluid Property Model With Application to Nanofluid Flow in a Parallel-Disk System—Part I: A New Thermal Conductivity Model for Nanofluid Flow," ASME J. Heat Trans., **134**(5), p. 051002.
[10] Paul, G., Chopkar, M., Manna, I., Das, P. K., 2010, "Techniques for Measuring the Thermal Conductivity of Nanofluids: A Review," Renewable Sustainable Energy Rev., **14**, pp. 1913–1924.
[11] Assael, M., Antoniadis, K., and Wakeham, W., 2010, "Historical Evolution of the Transient Hot-Wire Technique," Int. J. Thermophys., **31**, pp. 1051–1072.
[12] Gross, U., Song, Y., and Hahne, E., 1992, "Thermal Conductivity of the New Refrigerants R134a, R152a, and R123 Measured by the Transient Hot-Wire Method," Int. J. Thermophys., **13**, pp. 957–983.
[13] Hong, S. W., Kang, Y. T., Kleinstreuer, C., and Koo, J., 2011, "Impact Analysis of Natural Convection on Thermal Conductivity Measurements of Nanofluids Using the Transient Hot-Wire Method," Int. J. Heat Mass Transfer, **54**, pp. 3448–3456.
[14] Vadasz, J. J., Govender, S., and Vadasz, P., 2005, "Heat Transfer Enhancement in Nano-Fluids Suspensions: Possible Mechanisms and Explanations," Int. J. Heat Mass Transfer, **48**, pp. 2673–2683.
[15] Putra, N., Roetzel, W., and Das, S. K., 2003, "Natural Convection of Nano-Fluids," Heat Mass Transfer, **39**, pp. 775–784.
[16] Li, C. H., and Peterson, G. P., 2010, "Experimental Studies of Natural Convection Heat Transfer of $Al_2O_3$/DI Water Nanoparticle Suspensions (Nanofluids)," Adv. Mech Eng., **2010**, p. 742739.
[17] Ni, R., Zhou, S. Q., and Xia, K. Q., 2011, "An Experimental Investigation of Turbulent Thermal Convection in Water-Based Alumina Nanofluid," Phys. Fluids, **23**, p. 022005.
[18] Donzelli, G., Cerbino, R., and Vailati, A., 2009, "Bistable Heat Transfer in a Nanofluid," Phys. Rev. Lett., **102**, p. 104503.
[19] Corcione, M., 2011, "Rayleigh-Bénard Convection Heat Transfer in Nanoparticle Suspensions," Int. J. Heat Fluid Flow, **32**, pp. 65–77.
[20] Hwang, K. S., Lee, J., and Jang, S. P., 2007, "Buoyancy-Driven Heat Transfer of Water-Based $Al_2O_3$ Nanofluids in a Rectangular Cavity," Int. J. Heat Mass Transfer, **50**, pp. 4003–4010.
[21] Kim, J., Kang, Y. T., and Choi, C. K., 2004, "Analysis of Convective Instability and Heat Transfer Characteristics of Nanofluids," Phys. Fluids, **16**, pp. 2395–2401.
[22] Tzou, D. Y., 2008, "Thermal Instability of Nanofluids in Natural Convection," Int. J. Heat Mass Transfer, **51**, pp. 2967–2979.
[23] Jang, S. P., and Choi, S. U. S., 2004, "Role of Brownian Motion in the Enhanced Thermal Conductivity of Nanofluids," Appl. Phys. Lett., **84**, pp. 4316–4318.
[24] Das, S. K., Putra, N., Thiesen, P., and Roetzel, W., 2003, "Temperature Dependence of Thermal Conductivity Enhancement for Nanofluids," ASME. J. Heat Trans., **125**(4), pp. 567–574.
[25] Prasher, R., Bhattacharya, P., and Phelan, P. E., 2005, "Thermal Conductivity of Nanoscale Colloidal Solutions (Nanofluids)," Phys. Rev. Lett., **94**, p. 025901.
[26] Chon, C. H., and Kihm, K. D., 2005, "Thermal Conductivity Enhancement of Nanofluids by Brownian Motion," ASME J. Heat Trans., **127**(8), p. 810.
[27] Murshed, S. M. S., Leong, K. C., and Yang, C., 2008, "Investigations of Thermal Conductivity and Viscosity of Nanofluids," Int. J. Therm. Sci., **47**, pp. 560–568.
[28] Mintsa, H. A., Roy, G., Nguyen, C. T., and Doucet, D., 2009, "New Temperature Dependent Thermal Conductivity Data for Water-Based Nanofluids," Int. J. Therm. Sci., **48**, pp. 363–371.
[29] Duangthongsuk, W., and Wongwises, S., 2009, "Measurement of Temperature-Dependent Thermal Conductivity and Viscosity of $TiO_2$-Water Nanofluids," Exp. Therm. Fluid Sci., **33**, pp. 706–714.
[30] Vajjha, R. S., and Das, D. K., 2009, "Experimental Determination of Thermal Conductivity of Three Nanofluids and Development of New Correlations," Int. J. Heat Mass Transfer, **52**, pp. 4675–4682.
[31] Teng, T. P., Hung, Y. H., Teng, T. C., Mo, H. E., and Hsu, H. G., 2010, "The Effect of Alumina/Water Nanofluid Particle Size on Thermal Conductivity," Appl. Therm. Eng., **30**, pp. 2213–2218.
[32] Turgut, A., Tavman, I., Chirtoc, M., Schuchmann, H., Sauter, C., and Tavman, S., 2009, "Thermal Conductivity and Viscosity Measurements of Water-Based $TiO_2$ Nanofluids," Int. J. Thermophys., **30**, pp. 1213–1226.
[33] Shima, P., Philip, J., and Raj, B., 2010, "Synthesis of Aqueous and Nonaqueous Iron Oxide Nanofluids and Study of Temperature Dependence on Thermal Conductivity and Viscosity," J. Phys. Chem. C, **114**, pp. 18825–18833.
[34] Lee, W. H., Rhee, C. K., Koo, J., Lee, J., Jang, S. P., Choi, S. U. S., Lee, K. W., Bae, H. Y., Lee, G. J., Kim, C. K., Hong, S. W., Kwon, Y., Kim, D., Kim, S. H., Hwang, K. S., Kim, H. J., Ha, H. J., Lee, S. H., Choi, C. J., and Lee, J. H., 2011, "Round-Robin Test on Thermal Conductivity Measurement of ZnO Nanofluids and Comparison of Experimental Results With Theoretical Bounds," Nanoscale Res. Lett., **6**, p. 258.
[35] Carslaw, H. S., and Jaeger, J. C., 1959, *Conduction of Heat on Solids*, Oxford University Press, New York, pp. 188–213.
[36] Roder, H. M., Perkins, R. A., Laesecke, A., and de Castro, C. A. N., 2000, "Absolute Steady-State Thermal Conductivity Measurements by Use of a Transient Hot-Wire System," J. Res. Natl. Inst. Stand. Technol., **105**, pp. 221–253.
[37] Kostic, M., and Simham, K. C., 2009, "Computerized, Transient Hot-Wire Thermal Conductivity (HWTC) Apparatus for Nanofluids," Proceedings of the 6th WSEAS International Conference on Heat and Mass Transfer (HMT'09).
[38] Codreanu, C., Codreanu, N., and Obreja, V., 2010, "Experimental Set-Up for the Measurement of the Thermal Conductivity of Liquids," Rom. J. Inf. Sci. Technol., **10**, pp. 215–231.
[39] Lee, S., and Kang, K., 2007, "Validation Test for Transient Hot-wire Method to Evaluate the Temperature Dependence of Nanofluids," Trans. Korean Soc. Mech. Eng., B, **31**, pp. 341–348 (in Korean).
[40] Berendsen, H. J. C., 2011, *A Student's Guide to Data and Error Analysis*, Cambridge University Press, Cambridge, UK.
[41] Morkoç, H., and Özgür, Ü., 2009, *Zinc Oxide: Fundamentals, Materials and Device Technology*, Wiley-VCH, Weinheim, Germany.